

1 Introduction

2 Numerical Method

In this section we describes how we generate EMRI waveforms in non-Kerr metric and process EMRI signal. In 2.1, a continuously parametrized metric proposed by [5] is introduced, in 2.2, the method to generate EMRI waveforms proposed by [1] is described and 2.3 summarizes the signal processing pipeline.

2.1 Konoplya-Rezzolla-Zhidenko parametrization

In order to test Kerr hypothesis or General Relativity, one need an alternative theory or a non-Kerr metric. Here we use the metric parametrization proposed by Konoplya, Rezzolla and Zhidenko (see [5]) and still calculate the gravitational wave within General Relativity.

The line element around an axisymmetric black hole in KRZ parametrization is [5]:

$$ds^2 = \dots \quad (1)$$

Where the functions Y can be expanded by power series of $\cos \theta$. Here we use the same deformation parameter as [6], namely δ_i , $i = 1, 2, 3, 4, 5, 6$ related to the metric functions by

$$K = \dots \quad (2)$$

KRZ parametrization preserves stationarity and axisymmetry. When each δ_i is set to 0, the metric recovers Kerr metric.

2.2 "Kludge" Waveform

We use the method established in [1], i.e. Kludge waveform, to calculate EMRI waveforms. The procedure is: regarding the stellar mass object as a point particle, first calculate the trajectory of the particle in a given metric by integrating geodesic equations; then use quadruple formula to get the gravitational wave from geodesics.

In our instance, to calculate the geodesics, we use:

$$\dot{u}^\mu = -\Gamma_{\rho\sigma}^\mu u^\rho u^\sigma \quad (3)$$

$$\dot{x}^\mu = u^\mu \quad (4)$$

where x^μ is the Boyer-Lindquist coordinate of the particle, u^μ is the 4-velocity and $\Gamma_{\rho\sigma}^\mu$ is Christoffel connection. We didn't use conservation of particle mass, energy and angular momentum to reduce equation but to monitor numerical error. Namely at each step of integration, we check the conservation quantities defined by:

$$\eta = g_{\mu\nu} u^\mu u^\nu \quad (5)$$

$$E = -u_t = -g_{tt} u^t - g_{t\phi} u^\phi \quad (6)$$

$$Lz = u_\phi = g_{t\phi} u^t + g_{\phi\phi} u^\phi \quad (7)$$

and in Kerr cases, we also check Carter constant

$$Q = (g_{\theta\theta} u^\theta)^2 + \cos^2 \theta (a^2 (\eta^2 - E^2) + (\frac{Lz}{\sin \theta})^2) \quad (8)$$

During the calculation, we keep the relative drift of conserved quantities less than 10^{-7} .

e, p, ι

Transform (r, θ, ϕ) into (x, y, z) with the definition of spherical coordinate (rather than the Boyer-Lindquist coordinate), namely $x = r \sin \theta \cos \phi, y = r \sin \theta \sin \phi, z = r \cos \theta$. Then use quadruple formula and transform the waveform into transverse-traceless gauge (see formula (17) and (23) in [1]). With the resulted "plus" and "cross" components, we define our waveform as $h = h_+ + i h_\times$

2.3 Matched Filtering

3 Confusion Problem

When we try to identify EMRI signals, the confusion problem, as described in [3], could prevent us from discern non-Kerr signal and Kerr signal. Namely an overlap over 0.97 might happen between non-Kerr signals and Kerr ones with certain parameters. In 3.1 and 3.2 we show the confusion problem when matching EMRIs from equatorial and inclined orbit

3.1 Equatorial orbit

Given a waveform under spacetime with non-zero deformation parameter, in order to see if there is "confusion problem", we need to decide which waveform under Kerr spacetime is most similar to it and look at their overlap. Here we search for existence confusion problem with similar method as [2], i.e. looking at waveforms with same orbital frequency. The orbital frequencies in Kerr spacetime are given in [7]. In equatorial orbits, there are two frequencies ω_ϕ and ω_r related to motion of ϕ and r coordinates.

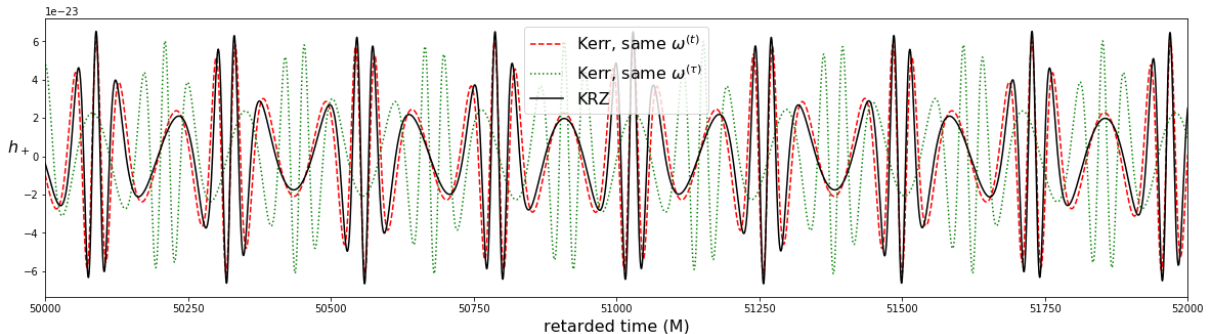


Figure 1: Comparison between waveforms of h_+ with respect to retarded time in units of central black hole mass M . The black solid line is the waveform under $\delta_1 = 0.2, e=0.5, p=6$. The red dashed line is the waveform under $\delta_1 = 0$ and e, p adapted so that the orbital frequencies with respect to t $\omega_r^{(t)}$ and $\omega_\phi^{(t)}$ are the same as that of the orbit under $d1=0.2, e=0.5, p=6$. The green dotted line is the waveform under $\delta_1 = 0$ and e, p adopted so that $\omega^{(\tau)}$ s are the same. The spin of the central black hole is $0.5M$.

If we restrict ourselves to equatorial motion, set the initial t and ϕ to 0 in view of stationarity and axisymmetry and set initial $r = r_{max}$, then the orbit is uniquely determined by orbital

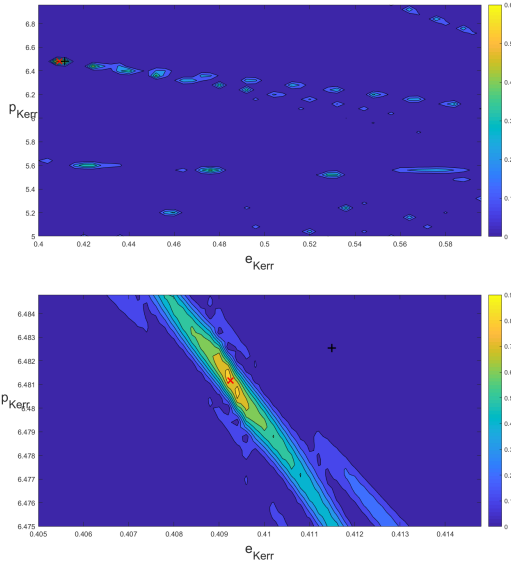


Figure 2: Distribution of overlap between waveform of $(\delta_1, a, M, e, p) = (0.2, 0.5, 2 \times 10^5, 0.5, 6)$ and waveforms of $(\delta_1, a, M, e, p) = (0, 0.5, 2 \times 10^5, e_{Kerr}, p_{Kerr})$ on (e_{Kerr}, p_{Kerr}) plane. Red cross mark: same $\omega^{(t)}$ at $(e_{Kerr}, p_{Kerr}) = (0.409248, 6.481170)$, overlap is 0.8912. The grid size is 50*50.

eccentricity e , semilatus rectum p , deformation parameters δ_i , BH mass M and BH spin a . As described in [2], we can achieve same orbital frequency as non-Kerr signal by varying orbital parameters e, p or BH parameters M, a . So we need to consider EMRIs determined by (δ, a, M, e, p) , $(0, a, M, e_{Kerr}, p_{Kerr})$ and $(0, a_{Kerr}, M_{Kerr}, e, p)$. Comparison of waveforms of same orbital frequency is shown in Fig. 1. The overlap between waveforms varying BH mass and spin is over 0.99. In fact, the geodesics that generate the two waves are overlapping.

According to Ref. [3], orbits with same orbital frequency ω_r and ω_ϕ can generate gravitational waveforms potentially confused with non-Kerr signals. Therefore the overlap between a non-Kerr waveform and several Kerr waveforms should have a local maximum around the parameter leading to same orbital frequency. Here we check this result by looking at overlaps between waveform of $(\delta_1, a, M, e, p) = (0.2, 0.5, 2 \times 10^5, 0.5, 6)$ and of $(\delta_1, a, M, e, p) = (0, 0.5, 2 \times 10^5, e_{Kerr}, p_{Kerr})$ with varying e_{Kerr} and p_{Kerr} . First we look at overlap distribution on a relatively large range of (e, p) . Then we search near (e_{Kerr}, p_{Kerr}) with same orbital frequency, as shown in Fig. 2.

Since metric deformation is more evident near BH horizon, we look at waveforms generated by trajectories close to innermost bound orbit. We compare waveforms of $(\delta_1, a, M, e, p) = (0.2, 0.5, 2 \times 10^5, e, p)$ and Kerr orbits varying (e, p) or (M, a) in a 50*50 grid of (e, p) . Contour plots of waveform overlap when varying (e, p) and (M, a) are shown in Fig. 3 and 4. The confusion problem exists when varying (M, a) for most region we considered.

Furthermore, the confusion problem exists for a large range of deformation parameter. When changing the deformation parameter, we found a almost linear relation between δ_i and varied BH spin/mass, a_{Kerr} and M_{Kerr} , as shown in Fig. 5. Fig. 6 shows that slope of this "linear"

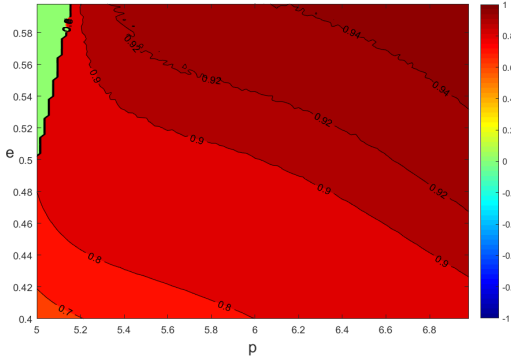


Figure 3: distribution of overlap between waveform of $(\delta_1, a, M, e, p) = (0.2, 0.5, 2 \times 10^5, e, p)$ and Kerr waveform with identical $\omega^{(t)}$ by varying e_{Kerr}, p_{Kerr} . The grid size is 50*50. The green region is unstable orbits.

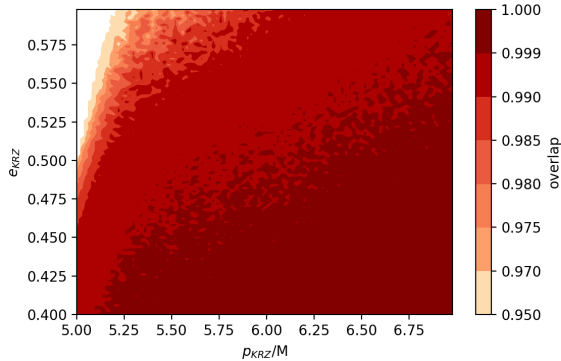


Figure 4: distribution of overlap between waveform of $(\delta_1, a, M, e, p) = (0.2, 0.5, 2 \times 10^5, e, p)$ and Kerr waveform with identical $\omega^{(t)}$ by varying M_{Kerr}, a_{Kerr} . The grid size is 50*50. The blank region is unstable orbits.

relation varies greatly for different (e, p) , so the relation is not a property intrinsic to the metric but dependent on the orbit. The linearity is not a result of small deformation. In fact, as shown in the two figures, the spin varies up to one or two times the spin in KRZ metric.

Therefore, for a given orbit parameter (e, p) , we can regard the introduction of δ_i as adding the black hole spin and mass proportionally. This sets an limit for the range of deformation parameters within which we can play the trick of varying (M_{Kerr}, a_{Kerr}) . The upper limit is set by requiring $a_{Kerr} < 1$ and the lower is limited by $a_{Kerr} > 0$ or stable orbit, e.g. for $(e, p) = (0.5, 6.0)$, when a_{Kerr} is small, the orbit is no longer stable and bounded. Fig. 7 shows the upper and lower bound of deformation parameters with respect to BH spin for orbit with $e = 0.5, p = 6.0$.

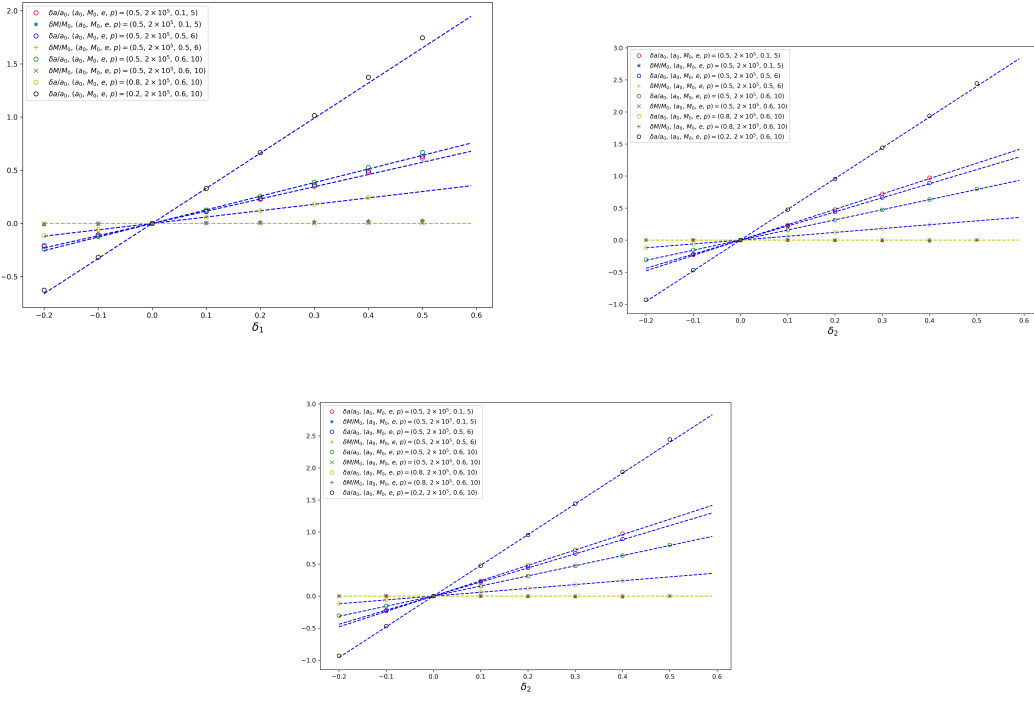


Figure 5: relation between relative varied spin/Mass and , for upper panel: δ_1 , for lower panel: δ_2 , when varying spin and mass to get identical $\omega^{(t)}$. The relative varied mass $\delta M/M_0$ is almost zero compared to relative varied spin $\delta a/a_0$. Moreover, $\delta a/a_0$ show linear behavior with respect to deformation parameters.

3.2 Inclined orbit

Equatorial orbits set some special conditions, i.e. number of orbital frequencies is equal to number of Kerr BH parameters. Therefore, in general we can solve mass and spin by the two frequency requirements set by KRZ orbit, and the resulted geodesics are almost identical. However, astrophysical EMRIs are usually generated by inclined orbits, which have three orbital frequencies. In such cases we usually cannot equate the three frequencies by only varying BH parameters.

However, we found that by varying (M, a, p) to equate three orbital frequencies, the resulted gravitational waveforms also have an overlap over 0.97, even though the orbits are apparently not identical. Upper and middle panel of Fig. 8 show the time series of motion in r, θ direction and trajectories in the last 5000s, the total time is 3×10^6 s. Motion at θ direction is almost overlapping with a few distortions. Motion at r direction has the same frequency but different amplitude, basically resulted from varying the semi-latus p . However, the gravitational wave signal are almost identical as shown in the bottom panel.

Similar to equatorial cases, requirements of $a_{Kerr} < 1$ and stable orbits set bound to the deformation parameters. However, since there's no carter-like constant in KRZ metric, we cannot

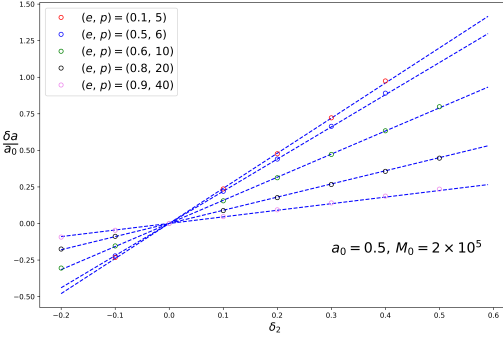


Figure 6: influence of (e, p) on the slope of the aforementioned linear relation between $\delta a/a_0$ and deformation parameter.

control orbit parameters (e, p, ι) . Therefore, we try just to control the initial condition so that the orbit parameter are at least near the desired value, e.g. $(e, p, \iota) = (0.2, 8, \pi/4)$. Technically, given δ_i , a_{KRZ} and reference orbit parameter, we calculate the energy E_{Kerr} and angular momentum L_{z-Kerr} in Kerr spacetime with spin equal to a_{KRZ} , then set the initial coordinate as $\theta = \pi/2$, $\phi = 0$, $t=0$ and r at $\frac{p}{1-e}$, set E, L_z equal to the Kerr value, which determines velocity in t and ϕ direction, set $u^r = 0$ and u^θ is determined by modulus of 4-velocity. The upper and lower bound of deformation parameters determined in this way is shown in Fig. 9. M_{KRZ} is 10^6 solar mass and total time is 2×10^6 s.

Note that the difference between equating $\omega^{(t)}$, orbital frequency with respect to coordinate time, and $\omega^{(\tau)}$, orbital frequency with respect to proper time, can be significant. From Fig. 2 it is explicit that the same orbital frequency with respect to t can result in almost the largest overlap while the same orbital frequency with respect to τ cannot. In Kerr spacetime, the expression for $\omega^{(t)}$ and $\omega^{(\tau)}$ are given in [4] and [7].

This result is explicit by looking at the waveforms over a relatively long time (here about $50000M$), as shown in Fig. 1.

Therefore we regard waveforms in Kerr spacetime with same orbital frequencies with respect to proper time as best matches to waveforms in non-Kerr space time under KRZ parametrization.

Fig. shows the overlap distribution...

As Fig. suggest, the confusion problem still exists in KRZ parametrization. In terms of gravitational waves, the deformation parameters are kind of degenerated with spin in Kerr spacetime. This resulted can also be found by looking at covariance matrix as discussed in next section

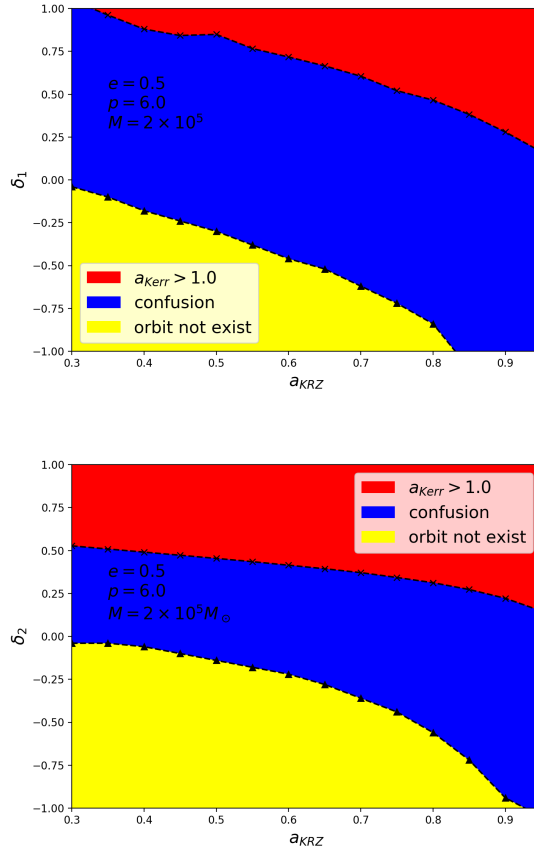


Figure 7: upper limit of deformation δ_2 for each spin, waveform of which parameter can be recovered by varying spin and mass under Kerr metric. The waveform have $(e, p)=(0.1, 6)$

4 Constraints on deformation parameter by future LISA task

References

- [1] Stanislav Babak, Hua Fang, Jonathan R. Gair, Kostas Glampedakis, and Scott A. Hughes. “kludge” gravitational waveforms for a test-body orbiting a kerr black hole. *Phys. Rev. D*, 75:024005, Jan 2007.
- [2] Enrico Barausse, Luciano Rezzolla, David Petroff, and Marcus Ansorg. Gravitational waves from extreme mass ratio inspirals in nonpure kerr spacetimes. *Phys. Rev. D*, 75:064026, Mar 2007.

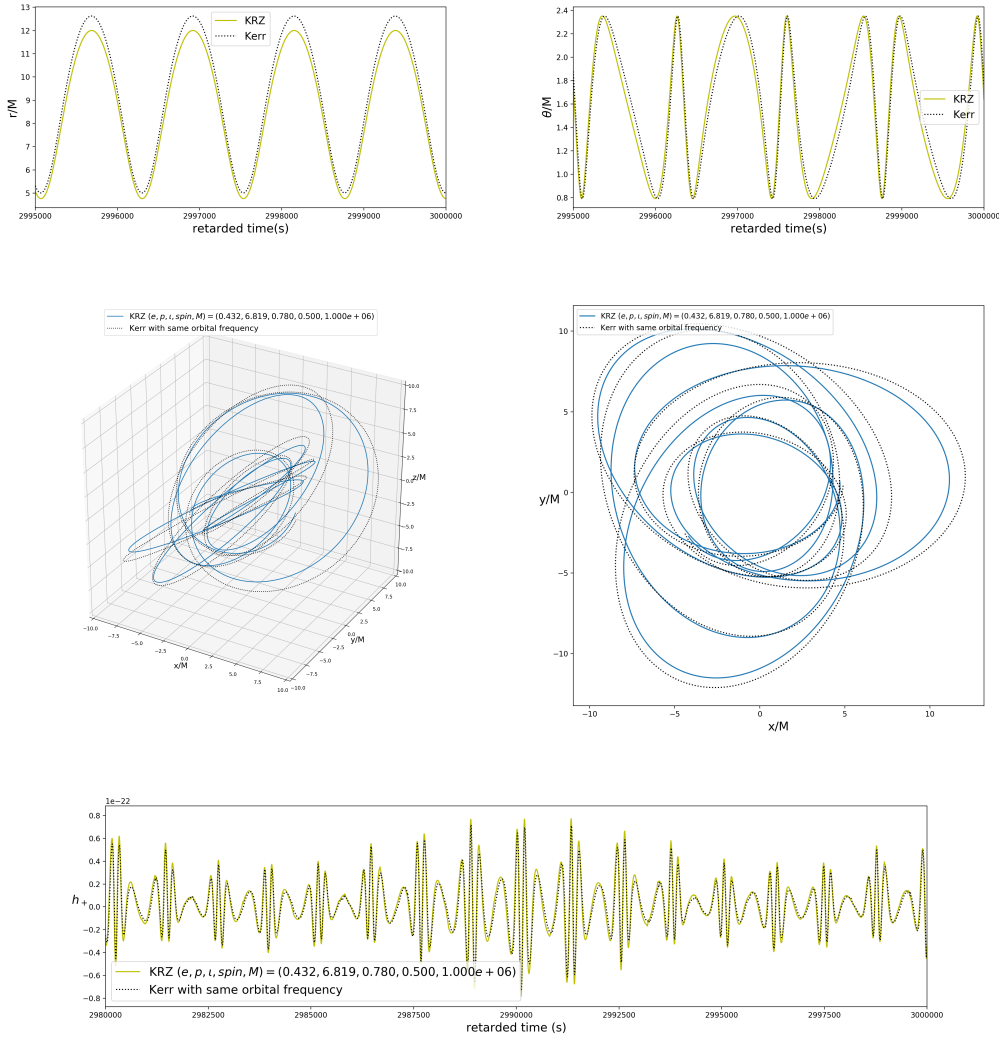


Figure 8: Orbits and GW waveforms of a KRZ orbit and a Kerr one with same orbital frequencies. Top left panel: time series of motion in r direction in last 5000s. Top right panel: time series of motion in θ direction in last 5000s. Middle left panel: trajectories in last 5000s. Middle right panel: projection on xy -plane of the trajectories in last 5000s. Bottom panel: "plus" component of EMRI waveform in last 20000s. The orbit parameters and BH spin/Mass are $(e, p, \iota, \text{spin}, M) = (0.432, 6.819, 0.780, 0.500, 1.000e + 06)$. The deformation parameter of the KRZ orbit is $\delta_1 = 0.2$.

- [3] Kostas Glampedakis and Stanislav Babak. Mapping spacetimes with lisa: inspiral of a test body in a 'quasi-kerr' field. *Classical and Quantum Gravity*, 23(12):4167, 2006.
- [4] Kostas Glampedakis and Daniel Kennefick. Zoom and whirl: Eccentric equatorial orbits around

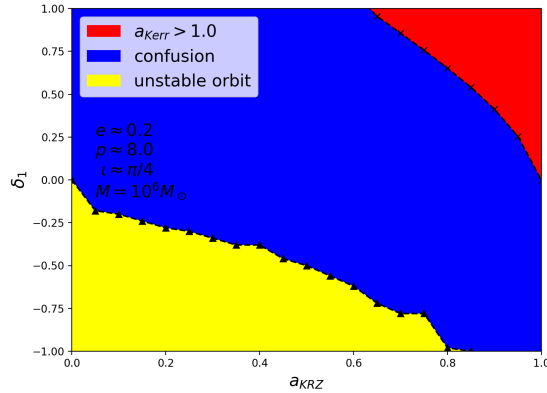


Figure 9: upper limit of deformation δ_2 for each spin, waveform of which parameter can be recovered by varying spin and mass under Kerr metric. The waveform have $(e, p)=(0.1, 6)$

spinning black holes and their evolution under gravitational radiation reaction. *Phys. Rev. D*, 66:044002, Aug 2002.

- [5] Roman Konoplya, Luciano Rezzolla, and Alexander Zhidenko. General parametrization of axisymmetric black holes in metric theories of gravity. *Phys. Rev. D*, 93:064015, Mar 2016.
- [6] Yueying Ni, Jiachen Jiang, and Cosimo Bambi. Testing the kerr metric with the iron line and the krz parametrization. *Journal of Cosmology and Astroparticle Physics*, 2016(09):014, 2016.
- [7] W Schmidt. Celestial mechanics in kerr spacetime. *Classical and Quantum Gravity*, 19(10):2743, 2002.